

A two species trap for chromium and rubidium atoms

Sven Hensler, Axel Griesmaier, Jörg Werner, Axel Görlitz and Tilman Pfau
5. Physikalisches Institut, Universität Stuttgart, 70550 Stuttgart (Germany)

October 30, 2018

Abstract

We realize a combined trap for bosonic chromium (^{52}Cr) and rubidium (^{87}Rb) atoms. First experiments focus on exploring a suitable loading scheme for the combined trap and on studies of new trap loss mechanisms originating from simultaneous trapping of two species. By comparing the trap loss from the ^{87}Rb magneto-optical trap (MOT) in absence and presence of magnetically trapped ground state ^{52}Cr atoms we determine the scattering cross section of $\sigma_{inelRbCr} = 5.0 \pm 4.0 \cdot 10^{-18} \text{ m}^2$ for light induced inelastic collisions between the two species. Studying the trap loss from the Rb magneto-optical trap induced by the Cr cooling-laser light, the photoionization cross section of the excited $5\text{P}_{3/2}$ state at an ionizing wavelength of 426 nm is measured to be $\sigma_p = 1.1 \pm 0.3 \cdot 10^{-21} \text{ m}^2$.

1 Introduction

The dominant interaction in atomic Bose-Einstein condensates (BEC) realized so far, is the contact interaction. In the ultracold regime, this interaction is isotropic and short range. Recently, increasing theoretical interest has focused on the dipole-dipole interaction [1, 2, 3]. This interaction is long range and anisotropic and thus would greatly enrich the physics of degenerate quantum gases. Additionally, tuning of this interaction from attraction to repulsion is possible by applying time dependent external fields [4]. Together with the use of a Feshbach resonance to vary the s-wave scattering length this would allow control of the scattering properties of an ultracold sample over a wide range of values and characteristics.

A promising candidate for the observation of the influence of the dipole-dipole interaction on the dynamics of a BEC is atomic chromium [5]. Due to its comparably large magnetic dipole moment of $6\mu_B$, where μ_B is the Bohr magneton, the dipole-dipole interaction is of the same order of magnitude as the contact interaction. However, many of the effects proposed for dipolar gases [6, 7, 8] require a much stronger dipole-dipole interaction. Magnetic dipole moments or electric dipole moments aligned in external fields that lead to such strong dipolar interaction can be found in heteronuclear molecules. The strongly paramagnetic Cr-Rb-molecule, is thus expected to have a large electric dipole moment beside its magnetic moment. In addition, the generation of degenerate gases of ultracold Cr-Rb-molecules formed by two ultracold gases of Cr and Rb

which are each produced by laser cooling and subsequent sympathetic cooling [9] seems to be feasible.

The paper is organized as follows. After a short description of our experimental setup, we present our findings on photoionization of the excited Rb^* . Measurements concerning interspecies collisions can be found in the subsequent section followed by our conclusions.

2 The combined magneto-optical trap for Cr and Rb

As a first step, on the way to the generation of ultracold, heteronuclear molecules, we have realized a two species magneto-optical trap for chromium and rubidium atoms. For our measurement we prepare both MOTs in the quadrupole field of two coils oriented in anti-Helmholtz configuration. Each trap is formed by three orthogonal and retro-reflected trapping laser beams, with the typical $\sigma^+ - \sigma^-$ -polarization. The trapping beams of the two traps are tilted by a small angle with respect to each other to be able to set up separate optics for both traps. We load about $N_{\text{Cr}} = 4 \cdot 10^6$ bosonic ^{52}Cr -atoms from a high temperature effusion cell via a Zeeman-slower into the Cr-MOT. The 426 nm cooling light is generated by a frequency doubled Ti:Sa-laser. The Rb-MOT with a steady state atom number of about $N_{\text{Rb}} = 3 \cdot 10^6$ Rb-atoms is loaded from the Rb-background gas provided by a continuously operated Rb-getter source. The stabilized Rb-cooling and repumping lasers are provided via a fiber from a different experimental setup. Both frequencies separated by 6.8 GHz are amplified by a single laser diode using injection locking technique. When both traps are operated at the same time, the steady state number of Rb atoms N_{Rb} drops by a factor of 5 due to photoionization of the excited Rb-cooling state.

3 Photoionization of magneto-optically trapped rubidium atoms

Photoionization of a neutral atom is a transition from a bound state $|i\rangle$ with internal energy E_i to a continuum state $|f\rangle$. Such a transition becomes possible if the energy $E_p = \hbar\omega_p$ of an incident photon exceeds the ionization-energy $E_{\text{ion}} = \hbar\omega_{\text{ion}}$ of the bound state $|i\rangle$. The transition rate $\Gamma_{i \rightarrow f}$ is given by Fermi's Golden Rule:

$$\Gamma_{i \rightarrow f} = \frac{2\pi}{\hbar} \left| \langle f | \hat{H}_{ia} | i \rangle \right|^2 \rho(E_i + E_p), \quad (1)$$

where $\langle f | \hat{H}_{ia} | i \rangle$ is the transition matrix element of the interaction Hamiltonian \hat{H}_{ia} and $\rho(E_i + E_p)$ is the density of states in the continuum at the final energy $E_i + E_p$. The photoionization rate can also be expressed using the photoionization cross-section $\sigma(\omega_p)$ if we define the photon-flux $\Phi = \frac{I_p}{\hbar\omega_p}$ using the intensity I_p of the ionizing light with a frequency of ω_p :

$$\Gamma_{i \rightarrow f}(\omega_p, I_p) = \sigma_p(\omega_p)\Phi \quad (2)$$

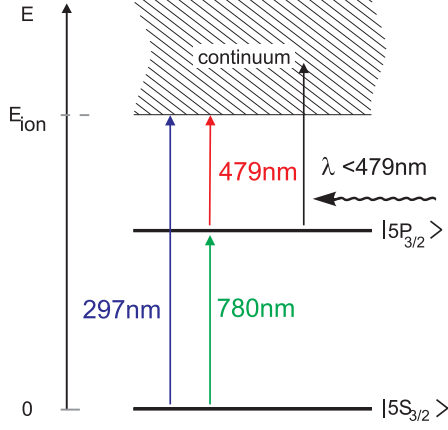


Figure 1: Energy diagram of the photoionization of Rubidium: The energy of the incident photon is sufficient to ionize the excited $5P_{3/2}$ state. The $5S_{1/2}$ ground state is unaffected. Above E_{ion} the possible final states form a continuum of states.

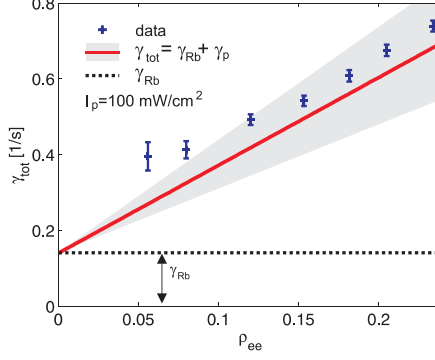


Figure 2: Dependence of the one body loss rate of the Rb trap on the population ρ_{ee} of the excited $5P_{3/2}$ state at an intensity of the ionizing laser of 100 mW/cm^2 . Note, the straight line is not a fit to the data, it is a calculated line using the mean value $\sigma_p = 1.1 \pm 0.3 \cdot 10^{-21} \text{ m}^2$ and the experimental parameters, where the error of σ_p is indicated by a grey area. The dotted line represents the mean of the measured pure background loss rates γ_{Rb} .

For ^{87}Rb the ionization threshold is at an energy level of 4.2 eV (297 nm) above the $5S_{1/2}$ ground state. With an energy difference of 1.6 eV (780 nm) between the ground state and the $5P_{3/2}$ excited state, the ionization energy of the excited state is 2.6 eV (479 nm). Thus, if we apply the Cr cooling laser (426 nm) in the Rb-MOT, transitions of excited Rb^* atoms to continuum states become possible. This situation is displayed in figure 1. During the process, energy and momentum are conserved and the excess energy is distributed among the electron and the ion leading to a velocity of the electron of $v_e \approx 3.4 \cdot 10^5 \text{ m/s}$. Therefore, recombination within the trap volume is very unlikely. Ions and electrons are not supported by the trap. This additional loss contributes to the total one-body loss rate, which reads $\gamma_{tot} = \gamma_{Rb} + \gamma_p$, where γ_p is the loss rate induced by the ionization and γ_{Rb} represents all other one body losses which are mainly caused by background gas collisions. As the ionization occurs in the excited state, the ionization rate $\Gamma_{i \rightarrow f}$ has to be multiplied with the population probability ρ_{ee} of the excited state:

$$\gamma_p = \Gamma_{i \rightarrow f} \rho_{ee} \quad , \text{ where} \quad (3)$$

$$\rho_{ee} = \frac{s}{2(s+1)}, \quad s = \frac{\langle C \rangle^2 I / I_s}{1 + (2\delta/\Gamma)^2}. \quad (4)$$

Here s is the saturation parameter expressed by the average Clebsch-Gordan coefficient $\langle C \rangle^2 = 7/15$, Γ the natural linewidth and $I_s = 1.6 \text{ mW/cm}^2$ the saturation intensity of the Rb trapping transition in a light field with total intensity I and detuning δ .

Neglecting two and three-body losses, which is a good approximation for the low densities we observe in our trap, the time evolution of the atom number $N_{Rb}(t)$ in the rubidium trap can be described by the following well known rate equation:

$$\frac{dN_{Rb}}{dt} = L - \gamma_{tot}N_{Rb}, \quad (5)$$

where L is the loading rate. We record loading curves of the Rb-MOT with a photodiode at different intensities of the Rb-MOT beams ranging from 20 mW/cm^2 to 160 mW/cm^2 and intensities of the Cr trapping light from 0 mW/cm^2 to 600 mW/cm^2 and determine the total loss rate γ_{tot} under each of these conditions. In figure 2 the measured loss rate γ_{tot} is plotted over ρ_{ee} at a total intensity of the ionizing laser of $I_p = 100 \text{ mW/cm}^2$. Subtracting the background loss rate γ_{rb} obtained from loading curves with no ionizing light present from the total loss rate, we extract the ionization rate $\gamma_p(I_{Rb}) = \gamma_{tot}(I_{Rb}) - \gamma_{Rb}$. The ionization rate shows a linear increase with the excited state population and vanishes for $\rho_{ee} \rightarrow 0$. We therefore attribute the increase of the one-body loss rate when the 426 nm Cr-trapping light is switched on to photoionization of excited Rb* atoms.

The population of the excited state is calculated using Eq. (4) and the intensities of the beams which are measured outside the chamber and corrected taking into account the transmission of the windows and the retroreflected beams. The Rb-MOT laser is tuned to maximum intensity of the fluorescence of the MOT, suggesting a detuning¹ of $\delta \approx 2.25 \pm 0.25\Gamma$. We estimate a total systematic error caused by the uncertainty in the detuning and spatial inhomogeneity of the laser beams of 20%. For each intensity of the Rb MOT beams a least square linear fit of Eq. (2) to the measured rate constants $\Gamma_{i \rightarrow f} = \gamma_p/\rho_{ee}$ yields σ_p . The mean value of these photoionization cross sections of the $5P$ state of ^{87}Rb at a wavelength of 426 nm is:

$$\sigma_p(426\text{nm}) = 1.1 \pm 0.3 \cdot 10^{-21} \text{m}^2 \quad (6)$$

This value is in good agreement with previously published values [14, 15] at comparable wavelengths and with theoretical predictions [16].

4 Inelastic interspecies collisions

In the second part of this article, we investigate the inelastic trap losses in combined Cr-Rb traps. During an interspecies collision in the presence of cooling light, each atom (Cr and Rb) undergoes several transitions from the ground to the excited state. If the atoms approach each other they experience a molecular potential. For ground state atoms the long-range part of this potential is dominated by the attractive van-der-Waals potential $V_{gg}(r) = C_6/r^6$, where r is the internuclear distance. Based on a two level model Schlöder et al. [17] pointed

¹According to several publications (see e.g. [13]) maximum fluorescence is observed at a detuning of $\delta \approx 2.25\Gamma$ and we estimated an accuracy of $\pm 0.25\Gamma$ of this value.

out, that this part of the molecular potential does not change its dependence on r if one of the atoms is in the excited state $V_{eg}(r) = C_6^*/r^6$. The C_6^* coefficient leads to an attractive (repulsive) interaction, if the excited atom has the smaller (larger) transition frequency of both the atoms. Since C_6^* is always larger than C_6 , the excited state potential is steeper. This has two consequences for Cr-Rb collisions:

First, inelastic collisions involving the excited state of Cr^* are prevented, because the steep, repulsive excited state potential hinders the two species to get very close to each other. Second, in contrast to homonuclear collisions, where the potential V_{eg} is proportional to r^{-3} , in the heteronuclear case, the colliding atoms decouple from the light field at smaller internuclear distances. This leads to a higher survival probability [18, 19], which means that the two atoms can approach each other in the Rb*-Cr-potential to a internuclear distance where fine structure changing collisions (FC) and radiative escape (RE) lead to trap losses.

Since loss due to photoionization of excited Rb-atoms triggered by the Cr-trapping light and loss due to Cr-light induced two-body collisions in the Cr-MOT [10] are dominant in both MOTs, it was not possible to observe trap loss due to interspecies collisions during the simultaneous operation of these traps. However, because of the 6 times larger magnetic moment of Cr we are able to prepare a magnetically trapped (MT) cloud of Cr-atoms and study the interaction with magneto-optically trapped Rb-atoms in the absence of the Cr-cooling light. As explained above, in a combined MOT for Cr and Rb we do not expect excited Cr atoms to contribute to the inelastic loss coefficient, therefore, the measured β -coefficient for inelastic collisions in the overlapped MT for Cr and MOT for Rb should be very similar to a coefficient measured while both MOTs are operated simultaneously.

For this measurement, we magnetically trap about $5 \cdot 10^7$ ^{52}Cr -atoms at $100 \mu\text{K}$ in the $^7\text{S}_3$ ground state using the continuous loading scheme presented by Stuhler et al. [11]. Here, the MT potential is created by the same coil configuration as described in the previous section. During the measurements the field gradient in the direction of the coil axis is 25 G/cm . Assuming a cut off parameter of $\eta = 10$ this results in a calculated magnetic trap depth of $k_B \cdot 530 \mu\text{K}$ for Cr-atoms in the extreme Zeeman substate [12]. We then apply the Rb cooling and repumping light for a certain interaction time t to load the Rb-MOT. The temperature of the Rb cloud is about $320 \mu\text{K}$. The light forces in the Rb-MOT result in a much deeper trapping potential of approximately $k_B \cdot 8 \text{ K}$. After the interaction time t the fluorescence of either the Rb-cloud or of the resonantly illuminated Cr-atoms is imaged onto a calibrated CCD-camera while no near resonant light is applied to the other species. The number of atoms of the imaged species is calculated from the pixel count of the image. We perform a series of such measurements in which we record the evolution of the number of Cr-atoms $N_{Cr}(t)$ and Rb-atoms $N_{Rb}(t)$. The temperature and the magnetic moment of the magnetically trapped Cr-Atoms are obtained from a 2D-fit to the atomic distribution in a quadrupole field under the influence of the gravity. The temperature of the Rb-atoms is deduced from the ballistic expansion of the cloud.

Figure 3 illustrates the decay of the number of magnetically trapped Cr-atoms during the first 30s with and without trapped Rb-atoms being present. Neglecting two-body loss, a fit of a one-body decay without trapped Rb-atoms

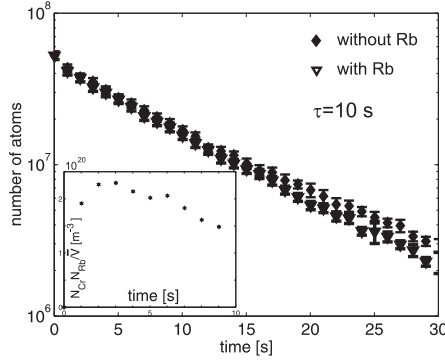


Figure 3: Decay of the number of magnetically trapped Cr-atoms with and without the influence of the Rb-MOT. The inset indicates the constants of the factor $N_{Cr}N_{Rb}/\bar{V}$.

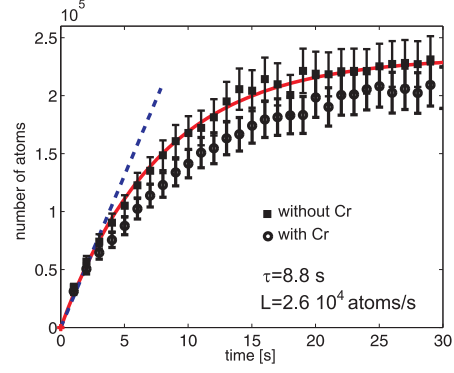


Figure 4: Loading curve of the Rb-MOT in the presence and absence of magnetically trapped Cr-atoms. The solid line indicates a fit of the one-body loading equation to the measurement without magnetically trapped Cr-atoms. The dotted line represents the initial slope of this fit.

present yields a lifetime of 10s. In the presence of the Rb-MOT the atom number is reduced by $8 \cdot 10^5$ atoms (25%) after 30s.

The loading process of the Rb-MOT is documented in figure 4. The measurement is performed with and without magnetically trapped Cr-atoms. Neglecting two- and three-body processes, we obtain a loading rate of $L_{Rb} = 2.6 \cdot 10^4$ atoms/s and a lifetime of 9s from a fit of the one-body loading equation to the data without trapped Cr-atoms. This yields a steady-state atom number of $2.3 \cdot 10^5$ atoms. The additional loss channel introduced by magnetically trapped Cr-atoms can be clearly observed.

The decay of the number of magnetically trapped Cr-atoms $N_{Cr}(t)$ and the increase of magneto-optically trapped Rb-atoms $N_{Rb}(t)$ during loading in the presence of the other species is governed by the following coupled rate equations:

$$\frac{dN_{Cr}}{dt} = -\gamma_{Cr}N_{Cr} - \beta_{CrRb} \int d^3r n_{Cr}n_{Rb} \quad (7)$$

$$\frac{dN_{Rb}}{dt} = L_{Rb} - \gamma_{Rb}N_{Rb} - \beta_{RbCr} \int d^3r n_{Cr}n_{Rb} \quad (8)$$

Because of the different loss channels of the two types of traps, β_{CrRb} and β_{RbCr} are not expected to be equal. The integral over both density distributions in the interspecies collision term can be approximated by the following expression [20]:

$$\int d^3r n_{Cr}n_{Rb} = \frac{N_{Cr}N_{Rb}}{\bar{V}}, \quad (9)$$

$$\bar{V} = V_{MT}/\varsigma, \quad (10)$$

$$\varsigma = e^{\frac{\bar{\sigma}^2}{2z^2}} \left(\frac{\bar{\sigma}^2}{z^2} + 1 \right) \left(1 - \text{Erf} \left[\frac{\bar{\sigma}}{\sqrt{2z}} \right] \right) - \sqrt{\frac{2}{\pi}} \frac{\bar{\sigma}}{z}, \quad (11)$$

where the effective collision volume \bar{V} varies between the Cr-MT volume $V_{MT} = 8\pi z^3$ for $\bar{\sigma} \ll z$ and the volume of the Rb-MOT V_{MOT} for $\bar{\sigma} \gg z$. The magnetic trap and the MOT are regarded to be isotropic with a $1/e$ -length z for the Cr cloud in the MT in direction of the coils axes and a mean $1/\sqrt{e}$ -size $\bar{\sigma}$ for the Rb-cloud in the MOT, respectively.

In order to deduce the loss coefficient β_{RbCr} from the Rb loading curve, Eq. (8) is solved for the first seconds by assuming a constant factor $N_{Cr}N_{Rb}/\bar{V}$ which is well reproduced by our data due to the inverse evolution of the atom numbers (see inset figure 3). From the initial slope α , the loss coefficient β_{RbCr} can be calculated:

$$\alpha = L_{Rb} - \beta_{RbCr} \frac{N_{Cr}N_{Rb}}{\bar{V}}. \quad (12)$$

Using L_{Rb} from the measurements in which no Cr-atom was trapped we obtain a loss coefficient of $\beta_{RbCr} = 1.4 \pm 1.1 \cdot 10^{-17} \text{ m}^3/\text{s}$ with a population probability of the excited Rb state of about 25%. This yields an inelastic cross section of $\sigma_{inel,RbCr} = \beta_{RbCr}\bar{v} = 5.0 \pm 4.0 \cdot 10^{-18} \text{ m}^2$, where we have used the mean velocity $\bar{v} = \sqrt{\frac{8k_B}{\pi} \left(\frac{T_{Cr}}{m_{Cr}} + \frac{T_{Rb}}{m_{Rb}} \right)}$. Due to uncertainties in N_{Cr} , N_{Rb} and \bar{V} we estimate a relative systematic error of 80%.

From the difference in the number of Cr atoms in the presence and absence of the trapped Rb cloud, we extract an upper and lower limit for the loss coefficient taking the maximum and minimum value of the factor $N_{Cr}N_{Rb}/\bar{V}$ and assuming this factor to be constant over the first 30 s: $4.7 \cdot 10^{-16} \text{ m}^3/\text{s} < \beta_{CrRb} < 5.5 \cdot 10^{-15} \text{ m}^3/\text{s}$. For this approximation we used the data points between 20 s and 30 s, where the data are well separated. The systematic relative error of these limits is again about 80%. The loss coefficients β_{RbCr} and β_{CrRb} we obtain, thus, differ by one order of magnitude. We attribute this to the large difference of the trap depths of the dissipative Rb-MOT and the conservative Cr-MT. Losses arise if the energy gained by inelastic collisions between unpolarized Rb and polarized Cr atoms is sufficiently high to eject an atom from its trap. Due to energy and momentum conservation 63% of the released energy is transferred to the Cr atoms. While in the Rb-MOT only fine structure changing (FC) and radiative escape (RE) interspecies collisions lead to additional trap loss, in the shallow Cr-MT FC, RE and hyperfine changing collision in the Rb atom, interspecies dipolar relaxation and depolarizing collisions which end in un-trapped states reduce the Cr atom number.

The atom loss in the Cr-MT in the presence of the Rb-MOT is accompanied by a temperature increase ($\sim 8 \mu\text{K}$) of the Cr cloud. Figure 5 depicts the evolution of the temperature with and without the presence of the other species. Without Rb atoms present, this heating rate is reduced to $4 \mu\text{K}/\text{s}$ and is mainly caused by anti-evaporation due to Majorana losses in the Cr-trap. We exclude thermalization with the Rb-MOT as the cause of the additional heating, because the same heating rate of the Cr cloud was measured in Cr traps prepared at temperatures lower and higher than the temperature of the Rb-MOT. Since the cloud is not collisionally dense, the atoms are expelled from the trap without depositing any energy in the cloud after most inelastic processes. Therefore, we attribute this increase to anti-evaporation caused by the mentioned loss mechanism within an inhomogeneous gas of Rb atoms and to collisions which lead to depolarization of the magnetic sublevels. In latter collisions, the energy difference between the substates of Cr and Rb (Rb*) which is $3/2\mu_B B$ ($4/3\mu_B B$)

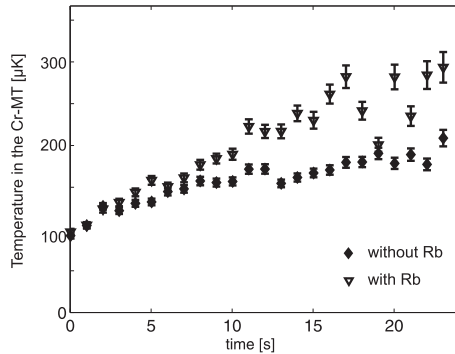


Figure 5: Temperature increase of the Cr-cloud in the MT. Depicted is the temperature evolution of the cloud in presence and absence of the Rb-MOT

in the small magnetic field near the trap center, is released and heats up the cloud.

5 Conclusions

The first results on a combined Cr-Rb trap which are presented in this paper show that the operation of both MOTs is limited by the photoionization of the excited state of the Rb-atoms which occurs with a cross section of $\sigma_p = 1.1 \pm 0.3 \cdot 10^{-21} \text{m}^2$. Due to other dominant loss mechanisms interspecies collisions could not be directly observed in the combined MOTs. By overlapping the Rb-MOT and the Cr-MT in space and time, we measured light induced interspecies collisions with a cross section of $\sigma_{inel, RbCr} = 5.0 \pm 4.0 \cdot 10^{-18} \text{m}^2$, in the Rb-MOT. Since collisions involving the excited state of Cr are prevented in a combined MOT of Rb and Cr atoms, a very similar cross section is expected for light induced collisions in a combined MOT. Due to the contribution of additional loss channels, the loss rate of Cr-atoms in the very shallow MT is more pronounced. Simultaneous operation of both MOTs could be improved by alternating cooling laser pulses for the two species which would suppress photoionization. If a Rb ground state trap is prepared before the Cr-MOT is loaded, light-induced interspecies collisions could be prevented.

The discussed measurements have already indicated the richness of the interaction in a combined system of trapped Cr and Rb atoms. An improvement of our Rb-source should allow us to load a significant number of Rb-atoms into a Rb-MT and study ground state collisions. These measurements will allow us to extract the elastic and inelastic interspecies ground state cross sections which are important for sympathetic cooling. Here, studies of inelastic processes resulting from the interaction of two species with very different internal structures are of theoretical interest to gain a deeper understanding of these relaxation processes.

6 Acknowledgment

We thank Axel Grabowski for providing us with stabilized Rb trapping light, K. Rzążewski and J. Stuhler for fruitful discussions. This work was funded by the DFG SPP 1116 and the RTN network "Cold Quantum Gases" under the contract No. HPRN-CT-2000-00125.

References

- [1] Baranov M., Dobrek L., Góral K., Santos L., and Lewenstein M., 2002, *Phys. Scripta*, T102, 74 and reference therein.
- [2] Góral K., Rzążewski K., and Pfau T., 2001, *Phys. Rev. A.*, **63**, 033606.
- [3] Santos L., Shlyapnikov G. V., Zoller P., and Lewenstein M., 2000, *Phys. Rev. Lett.*, **85**, pp. 1791.
- [4] Giovannazzi S., Görlitz A., and Pfau T., 2002, *Phys. Rev. Lett.*, **89**, 130401.
- [5] Schmidt P. O., Hensler S., Werner J., Griesmaier A., Görlitz A., Pfau T., and A. Simoni, 2003, *Phys. Rev. Lett.*, **91**, 193201.
- [6] Pu H., Zhang W., and Meystre P., 2001, *Phys. Rev. A*, **87**, 140405.
- [7] DeMille D., 2002, *Phys. Rev. Lett*, **88**, 067901.
- [8] Baranov M. A., Mar'enko M. S., Rychkov V. S., and Shlyapnikov G.V., 2002, *Phys. Rev. A*, **66**, 013606.
- [9] Modugno G., Ferrari G., Roati G., Brecha R. J., Simoni A., and M. Inguscio, 2001, *Science*, **294**, 1320-1322.
- [10] Bradley C. C., McClelland J. J., Anderson W. R., and Celotta R. J., 2000, *Phys. Rev. A*, **61**, 053407.
- [11] Stuhler J., Schmidt P. O., Hensler S., Werner J., Mlynek J., and T. Pfau, 2001, *Phys. Rev. A*, **64**, 031405.
- [12] Luiten O. J., 1996, Reynolds M. W., and Walraven J. T. M., *Phys. Rev. A*, **53**, 381
- [13] Rapol U. D., Wasan A. and Natarajan V., 2001, *Phys. Rev. A.*, **64**, 023402.
- [14] Dinneen T. P., Wallace C. D., Tan K.-Y. N., and Gould P. L., 1992, *Opt. Lett.*, **17**, 1706-1708.
- [15] Fuso F., Ciampini D., Arimondo E., and Gabbanini C., 2000, *Opt. Com.*, **173**, 223-232.
- [16] Aymar M., Robaux O., and Wane S., 1983, *At. Mol. Opt. Phys*, **17**, p. 993-1007.
- [17] Schlöder U., Engler H., Schünemann U., Grimm R., and Weidemüller M., 1999, *Eur. Phys. J. D*, **7**, 331-340.

- [18] Gallagher A., and Pritchard D. E., 1989, *Phys. Rev. Lett.*, **63**, 957-960.
- [19] Weiner J., Bagnato V. S., Zilio S., and Julienne P. S., 1999, *Rev. Mod. Phys.*, **71**, 1-85.
- [20] J. Stuhler, 2001, PhD Thesis University of Konstanz, Konstanz.